IOSR Journal of Mechanical and Civil Engineering (IOSR-JMCE)
e-ISSN: 2278-1684,p-ISSN: 2320-334X, Volume 14, Issue 5 Ver. IV (Sep. - Oct. 2017), PP 56-73
www.iosrjournals.org

A pragmatic anisotropic Damage Fatigue Model Based on a failure criterion and its gradient

A. Manai[a, b] , H. Hassis[a], A. Ben hamida[b], Anouar Krairi[c]
a: University of Tunis El Manar, National Engineering school of Tunis, ENIT, LR-03-ES05 Civil Engineering Laboratory 1002, Tunis, Tunisie.
b: University de Pierre et Marie Curie, LR Institut Jean Le Rond D'Alembert : 4 Place Jussieu 75005 Paris France.
c- Department of Materials, Textiles and Chemical Engineering (MaTCh), Ghent University, Technologiepark 903, 9052 Zwijnaarde, Belgium.

Abstract: *A new practical engineering methodology for the analysis of structures under cyclic loading is proposed in this work. A new anisotropic fatigue damage model is developed. The evolution of material properties degradation depends on a failure criterion and its gradient. The anisotropic material degradation will guide the damage propagation. The propagation of damage is mainly depending on the ridges of the criterion's "surface" (zero gradients). The proposed approach can describe the initiation and propagation of the damage until the structural failure under fatigue loading. For each finite element, a non-homogeneous anisotropic distribution of material properties are associated. Schematically, it seems like a material "surfing" on the criterion's "surface" and damages follow the crest of the criterion's "surface" (level and gradient). A global approach criterion, based on invariants of the stress tensor, is adopted. The reduction of material properties is assigned to a number of cycles and a global level of stresses, using an experimental Wöhler curve. Two simplified forms of the model are proposed and results are compared with a cruciform experimental reference example and an industrial case. A mapping with Dang Van criterion is also computed to analyze the numerical results.*

Key words*: Damage fatigue, failure criterion, Wohler curve, Damage initiation and propagation.*

Date of Submission: 12 -10-2017 Date of acceptance: 27-10-2017

I. Introduction

Mechanical components, in engineering applications, are usually subjected to sudden fatigue failure under multi-axial loadings. Well-designed mechanical assemblies that can be operated for long time, need an accurate estimation of the fatigue lifetime of each component. In order to evaluate the fatigue lifetime under multi-axial stress, efficient and accurate methodologies are required.

Many multi-axial fatigue criteria have been proposed in the literature in the last century [1–9]. The criterion developed by Sines [4], Crossland [6] and Dang Van et al. [5] are well-known and can be considered as referral criteria. The first two belong to the invariance group and the third one is based on the average value concept. The invariant formula usually consists of quantities related to hydrostatic and deviatoric stresses. The use of these hypotheses leads to determine the initiation point of fatigue cracks, but not their propagation and orientations. Sines [4] and Papadopoulos et al. [7])analyzed the influence of different combinations of variable bending and torsion stresses on the fatigue lifetime of a structure. The Sines hypothesis showed satisfactory correlations with experimental results.

After the criterion definition that determines the initiation of the damage at the most stressed areas, it is important to develop a cumulative damage law. The most accepted cumulative damage approach is the one developed by Miner [10] due to its relative simplicity. Also, it is a close-enough approximation to reality to be of practical use. [11-16].

Finally, when the crack theories are not considered, the fatigue damage is considered as a global damage defined by the criterion which determines the initiation of damage. The damage accumulation is approximated by laws.

The damage propagation, until the structural failure, the eventual change of its direction, or the change of loading orientation, is not sufficiently understood.

The Material's fatigue under multi-axial loadings is an old and enigmatic subject, this paper aims to develop an approach for initiation, propagation and failure. Mainly we focus on understanding two very complex issues with a real impact on material's reliability estimation:

• The parameters summarizing the effect of multi-axial fatigue (through a criterion, a concept, a model...): The concept, the model will not only determine the damage initiation but it is also used to characterize its propagation.
• The cumulative damage laws (linear and nonlinear) determining the fatigue lifetime: it will not be related only to the number of cycles, but also to the multi-axial loading and its eventual direction or intensity changes.

In summary, the objective of this work is to:

- Establish a general approach that defines the damage initiation, propagation, and the structural failure. It is based on a chosen criterion, an experimental behavior as the Wöhler curve and a cumulative model. The proposed approach takes into account the anisotropic degradation phenomenon.
- Test this approach with some experimental data from the literature [10].

II. Description of the proposed approach

2.1 Introduction

Continuum Damage Mechanics (CDM) is employed in the proposed approach. The CDM approach is based on the concept of damage variable and effective stress introduced by Kachanov (1958) [28] and Rabotnov (1963) [29]. A scalar damage variable (D) is usually used to model isotropic damage following the works of Lemaitre and Chaboche [30], and Mazars [21]. For anisotropic damage mainly two classical ways were introduced by Murakami-Ohno and Chaboche. The first one, by Murakami and Ohno, [17, 18], uses a second-rank damage tensor and a net stress tensor through a net area definition. The effective stress-strain behavior is then obtained by a fourth-rank tensor. The second theory, by Chaboche, [19, 20], uses one effective stress tensor only, defined in terms of the macroscopic strain behavior, through a fourth-order non-symmetrical damage tensor.

The effective stress $(\tilde{\sigma})$ in the case of anisotropic damage is expressed as function of the Cauchy stress (σ) as follows:

$$\tilde{\sigma}_{ij} = \left(I - D\right)^{-1}_{ijkl} \sigma_{kl} \tag{5}$$

With D and I are the fourth order damage and identity tensors, respectively.

Hereafter, the anisotropic damage model based on a chosen criterion and its gradient, is presented.

2.2 Description of the anisotropic damage approach based on the criterion and its gradient
The main objective of this approach is to propose a model allowing:

- To describe the damage initiation and its propagation
- To give an estimation of the structure lifetime under a multi-axial variable loading (even in its spatial distribution).

It is also a way to approach the damage accumulation, the stress redistribution and the damage propagation until the structural failure.

Our approach is classified as a model based on the principle of equivalence (of strain, or stress or energy). The three equivalence principles do not give the same relation between the effective and the initial stiffness tensor. No physical argument favors the use of one principle over others, but it seems that the principle of energy equivalence, and this is our choice, is the most used in the literature [25].

After choosing an adequate criterion and an appropriate Wöhler curve, the material degradation will affect the area with satisfied failure criterion. The material degradation will be anisotropic and it depends on the criterion gradient. The anisotropic material degradation will guide the damage propagation, by an anisotropic redistribution of stresses.

In order to affect damage, principally to the area with satisfied criterion, a Heaviside function is used. An idea to overcome the discontinuity of the Heaviside function difficulty is then to find a continuous regular function which presents a similar behavior [26-27].
Using the previous considerations, the following material properties degradations (as a discrete evolution law) are proposed for an iterative procedure:

$$\begin{aligned} E_x^{i+1} &= E_x^i.\left[1 - g.C^i * \left(1 - \nabla_n \vec{C}^i.\vec{i}\right)\right] \\ E_y^{i+1} &= E_y^i.\left[1 - gC^i * \left(1 - \nabla_n \vec{C}^i.\vec{j}\right)\right] \\ E_z^{i+1} &= E_z^i.\left[1 - g.C^i * \left(1 - \nabla_n \vec{C}^i.\vec{k}\right)\right] \end{aligned} \quad (6)$$

$$\begin{aligned} \nu_{xy}^{i+1} &= \nu_{xy}^i \frac{\left[1 - g.C^i * \left(1 - \nabla_n \vec{C}^i.\vec{i}\right)\right]}{\left[1 - g.C^i * \left(1 - \nabla_n \vec{C}^i.\vec{j}\right)\right]}; \nu_{yx}^{i+1} = \nu_{yx}^i \frac{\left[1 - g.C^i * \left(1 - \nabla_n \vec{C}^i.\vec{j}\right)\right]}{\left[1 - g.C^i * \left(1 - \nabla_n \vec{C}^i.\vec{i}\right)\right]} \\ \nu_{xz}^{i+1} &= \nu_{xz}^i \frac{\left[1 - g.C^i * \left(1 - \nabla_n \vec{C}^i.\vec{i}\right)\right]}{\left[1 - g.C^i * \left(1 - \nabla_n \vec{C}^i.\vec{k}\right)\right]}; \nu_{zx}^{i+1} = \nu_{zx}^i \frac{\left[1 - g.C^i * \left(1 - \nabla_n \vec{C}^i.\vec{k}\right)\right]}{\left[1 - g.C^i * \left(1 - \nabla_n \vec{C}^i.\vec{i}\right)\right]} \\ \nu_{yz}^{i+1} &= \nu_{yz}^i \frac{\left[1 - g.C^i * \left(1 - \nabla_n \vec{C}^i.\vec{j}\right)\right]}{\left[1 - g.C^i * \left(1 - \nabla_n \vec{C}^i.\vec{k}\right)\right]}; \nu_{zy}^{i+1} = \nu_{zy}^i \frac{\left[1 - g.C^i * \left(1 - \nabla_n \vec{C}^i.\vec{j}\right)\right]}{\left[1 - g.C^i * \left(1 - \nabla_n \vec{C}^i.\vec{k}\right)\right]} \end{aligned} \quad (7)$$

E^i is the Young modulu's of the step i, ν^i is the Poisson ratio of the step i, C is the criterion function, $\nabla_n \vec{C}^i$ is the normalized gradient of the criterion function, the function g presents a behavior similar to the Heaviside function , $(\vec{i}, \vec{j}, \vec{k})$ are the (x,y,z) direction vectors .

1.1. Illustration by an academic example

As a preliminary and schematically example, let a simply supported rectangular plate submitted to a sinusoidal bending loading. A Sines [4] criterion is used. It has the following form:

$$C = \frac{\sqrt{J_{2a}} + B\sigma_{H,m}}{A} \leq 1 \; ; \; A = \tau_{-1}; \quad B = 2\frac{\tau_{-1}}{\sigma_0} - \frac{1}{\sqrt{3}} \quad (1)$$

Where

- τ_{-1}: is the fatigue limit in fully reversed torsion
- σ_0: is the fatigue limit in fully reversed axial loading
- J_2: is the second invariant of the deviatoric stress tensor
- $\sigma_{H,m}$: is the first invariant of the stress tensor

$$J_{2,a} = \frac{1}{6}\left[(\sigma_{1a} - \sigma_{2a})^2 + (\sigma_{2a} - \sigma_{3a})^2 + (\sigma_{3a} - \sigma_{1a})^2\right] \quad (2)$$

And

$$\sigma_{H,m} = \frac{1}{3}(\sigma_{1m} + \sigma_{2m} + \sigma_{3m}) \quad (3)$$

- σ_{ia}, i = 1,2,3, are the amplitudes of the principal stresses;
- σ_{im}, i = 1,2,3 are the mean principal stresses;

The criterion evolution is shown in figure 1.a. The gradient components are shown in figures 1.b and 1.c.

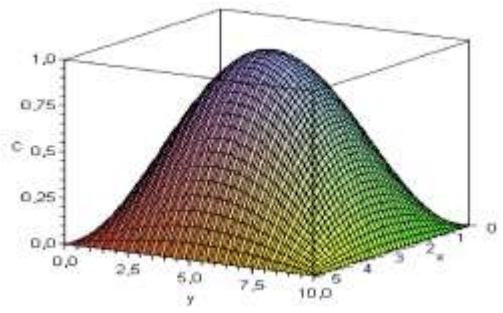

Figure 1.a. Space evolution of criteria C(x,y)

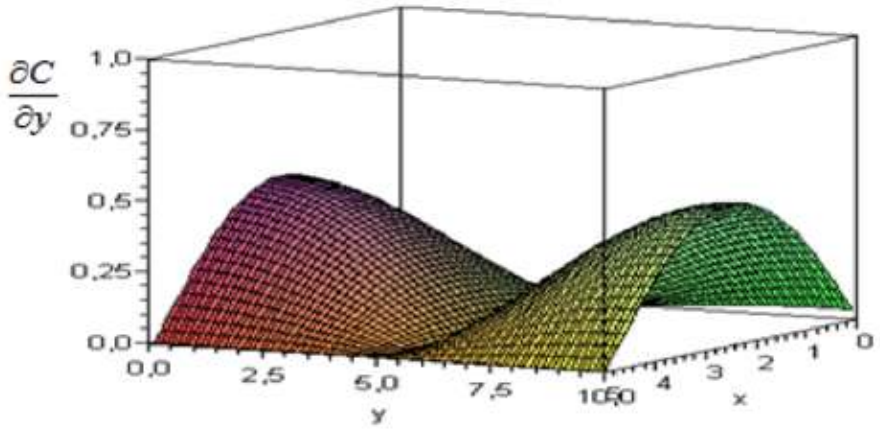

Figure 1.b. Space Evolution of the normalized criteria gradient (x component)

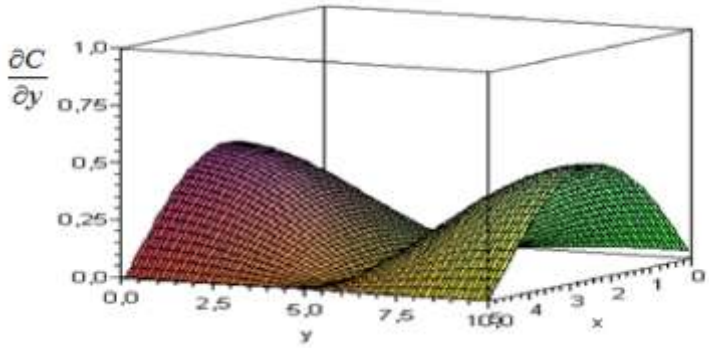

Figure 1.c. Space Evolution of the normalized criteria gradient (y component)

The degradation $\frac{E_x^{i+1}}{E_x^{i}}$ and $\frac{E_y^{i+1}}{E_y^{i}}$ ratio are represented in figures 1.d and 1.e, respectively.

The evolution of $\frac{\nu_{xy}^{i+1}}{\nu_{xy}^{i}}$ and $\frac{\nu_{yx}^{i+1}}{\nu_{yx}^{i}}$, Poisson ratio are represented in figures 1.f and 1.g, respectively.

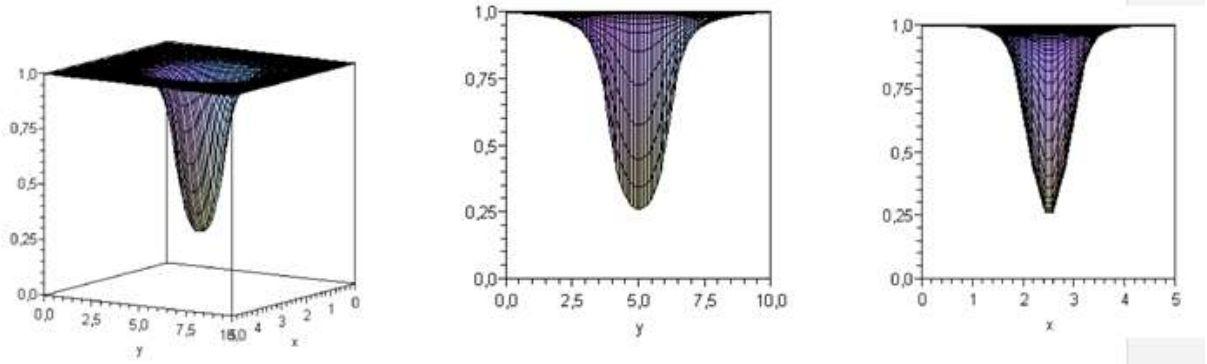

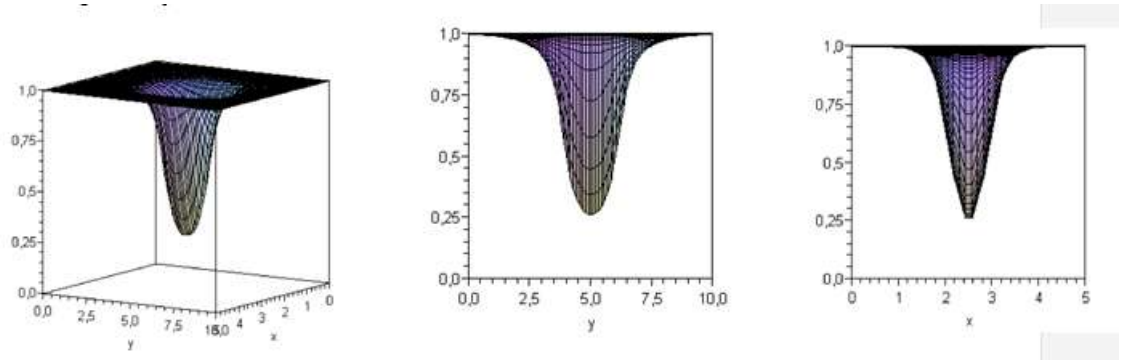

Figure 1.d. Degradation of the Young modulu's ratio $\frac{E_x^{i+1}}{E_x^i}$

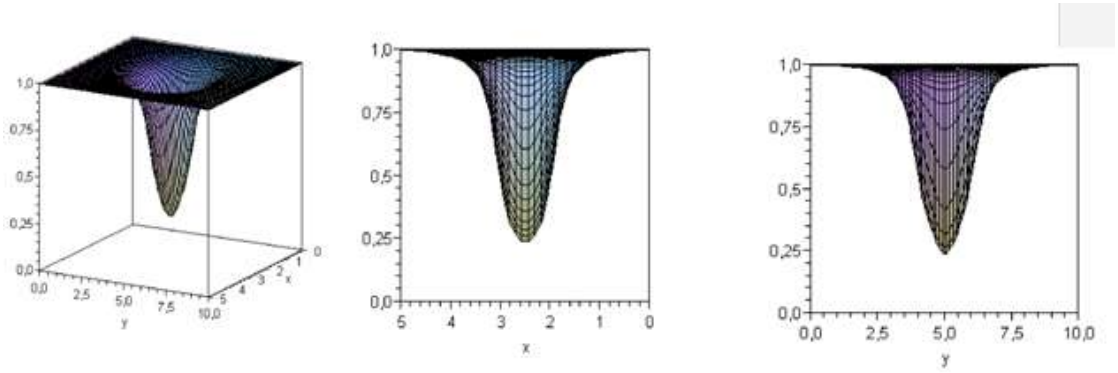

Figure 1.e. Degradation of the Young modulu's ratio $\frac{E_y^{i+1}}{E^i{}_y}$

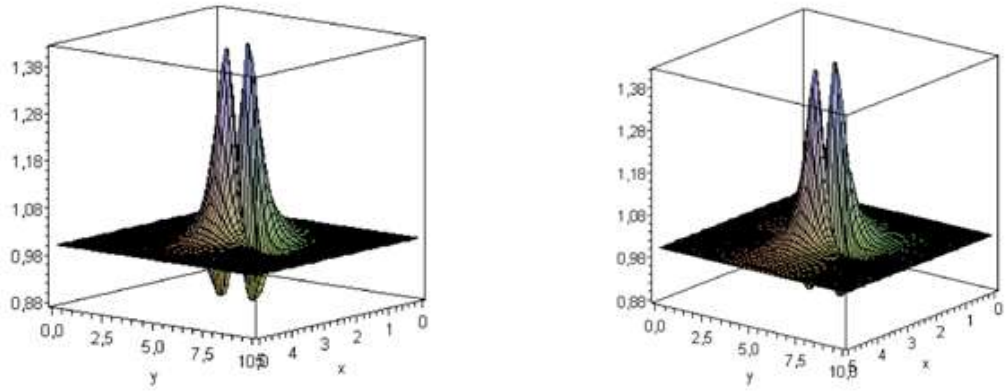

Figure 1.f. Evolution of $\frac{\nu^{i+1}{}_{xy}}{\nu^i{}_{xy}}$ Figure 1.g. Evolution $\frac{\nu^{i+1}{}_{yx}}{\nu^i{}_{yx}}$

2.3 Presentation of two simplified approaches

At the beginning of exploring this approach, the main problem is how to use the classical tools in computer codes to define the fatigue damage? And can we use a simplified model without any new tools?

Two simplified choices are adopted without the need for new computational developments:

- The first form of this approach consists in modeling damage by elimination of elements whose criterion is around 1 (here between 0.9 and 1).
- The second form consists in schematizing the damage by bilinear-elastic behavior with a low second stiffness. The damage is modeled by the decreased stiffness of the second elastic part. The stress at the beginning of the second elastic part is defined by the Wöhler curve. Each iteration decreases the stress at the beginning of the second elastic phase (following the Wöhler curve, as if it was performed a number of cycles and with the accumulation of linear damage). For the next iteration, the system is loaded by the deformation of the second elastic phase, in addition to the loading cycle.

The steps of the two simplified approaches are described as follows:

2.4.1. Steps for the first approach: "Elimination of damaged areas"

- **Initial step:**

✓ Determination of the initial state of stresses: $\sigma_0(\vec{x})$

✓ Choice of a criterion and a Wöhler curve

✓ Determination of the cycles required to initiate fatigue damage $N_0(\vec{x})$ witch correspond of the projection of the maximum criterion in the Wöhler curve.

- **From step 2 until the structural failure**

✓ Starting from the mapping stress of the previous iteration, $\sigma_{i-1}(\vec{x})$, and the number of cycles necessary to initiate the fatigue damage, $N_f^{i-1}(\vec{x})$, the damage distribution is defined using the chosen damage criterion, $C^{i-1}(\vec{x})$.

✓ The area with an index of damage $0.9 \leq C^{i-1}(\vec{x}) \leq 1$ is eliminated

✓ The next stress distribution, $\sigma_i(\vec{x})$, is determined, by a new computing elastic model with the damaged stiffness on the structure.

➢ The damage propagation is defined by the propagation of the damaged area (eliminated area)

➢ The structural failure is defined by a failure of the global stiffness structure. The calculation will be stopped automatically.

2.4.2. Steps for the second approach: "Degradation of the resistance of damaged area"

- **Initial step:**

Same step as the first approach

- **From step 2 until the structural failure**

✓ The stress at the beginning of the second elastic phase (the threshold) will follow (and decreases at each iteration) the Wöhler curve. This represents the successive material damage.

✓ A bi-linear elastic calculation is carried out for a one loading cycle

✓ The deformation of the second elastic phase is determined and it will be a load for the next iteration

✓ The stress at the beginning of the second phase decreases following the Wöhler curve; the deformation of the second elastic phase will be a loading, in addition to the cyclic loading. Redistribution of stresses will be made in a natural way.

✓ The propagation of the damage is defined by the propagation of the degraded areas represented by the deformation of the second elastic phase.

✓ The structural failure is defined by a failure of the stiffness of the structure. The calculation will be stopped automatically.

With these two forms of the simplified approaches, we can therefore determine:

• The area of damage initiation

• The damage propagation (following the damaged areas)

• The structural lifetime (by the structural failure)

2.5 Second approach with non-constant jumping cycles

In order to optimize the second simplified model, an iterative simulation is developed with a cycles jumping procedure, the jumping cycles (Δ N) is not constant. Statistical series are presented in table 1 where the random variable is the deformation of the second elastic phase and the effective is the surface of the elements.

- ε_{pi} : The deformation of the second elastic phase of the element i
- S_i: the surface of the element i

Random variable ε_p	ε_{p1}	ε_{p2}	ε_{p3}	…….	ε_{pn}
Effective : Element's surface	S_1	S_2	S_3	…..	S_n

Table 1. Random of the deformation of the second elastic phase

In order to determine the orientation of the damage propagation, iterations are performed with non-constant jumping cycles (Δ N) , defined as:

$$\Delta N = 2\frac{1-\Delta N_{max}}{\overline{\varepsilon_p}}\, s + \Delta N_{max} \quad (8)$$

With

- ΔN_{max} : Maximum jumping cycles
- $\overline{\varepsilon_p}$: Mean of deformation of the second elastic phase $\overline{\varepsilon_p} = \sum_{j=1}^{i} \frac{S_j\ \varepsilon_{pi}}{S_t}$
- The variation of the deformation of the second elastic phase $V = \sum_{j=1}^{i} \frac{S_j\,(\varepsilon_{pi} - \overline{\varepsilon_p})^2}{S_t}$
- S : Standard deviation of the deformation of the second elastic phase $s = \sqrt{V}$

The stress at the beginning of the second elastic phase is defined using the Wohler curve (Basquin model):

$$\sigma = \sigma_y = c\, N^a \quad (9)$$

c, a: Material parameters of the Wöhler Curve
σ_y : The stress at the beginning of the second elastic part.

The stress at the beginning of the second elastic phase decreases form N_i to N_{i+1}:

$$\sigma_y(N_{i+1}) = \sigma_y(N_i) + \Delta\sigma \quad (10)$$

With the first order of Taylor development, the stress deformation of the second elastic phase has the following expression:

$$\sigma_y(N_{i+1}) = \sigma_y(N_i) + \left.\frac{d\,\sigma_y}{d\,N}\right|_{N_i} \Delta N \quad (11)$$

$\Delta\sigma$: The stress variation
ΔN : The jumping cycles

III. Numerical applications

3.1 Academic example

To validate this approach, in its basic and simplified versions, a reference example was selected from the literature [10]. The considered example shows the relevance of our approach to achieve the detection of the fatigue damage initiation and its propagation, and eventually the monitoring of the fatigue damage until the whole structural failure.

For numerical results, the software CASTEM and ESI VPS software are used. To develop the approach in its final version, a specific development is needed.

3.2.1 Analyzed structure

The analyzed structure, shown in figure 2.a, is subjected to axial and biaxial loadings. In this analysis, only the fourth of the whole sample is investigated by imposing appropriate symmetry conditions (figure 2.b). The cruciform specimens are made of aluminum alloy (Al-6082-T6) with the mechanical properties presented in the table 2. The associated Wöhler curve used with the considered model is shown in figure 3. The cyclic loading applied is tension with frequency of 5Hz and a loading ratio $R = \frac{\sigma_{min}}{\sigma_{max}} = \frac{4}{40} = 0{,}1$.

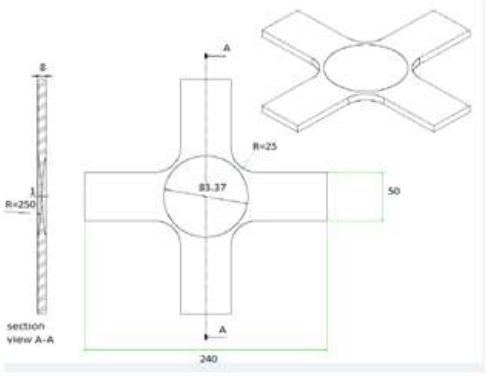

Figure 2.a: Analyzed structure [10]

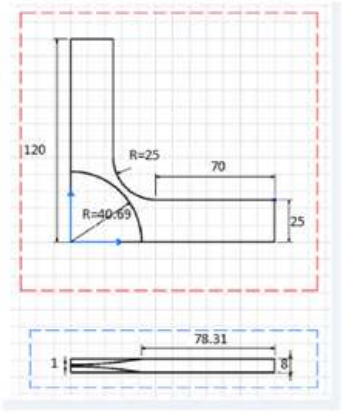

Figure 2.b: The ¼ analyzed structure [10]

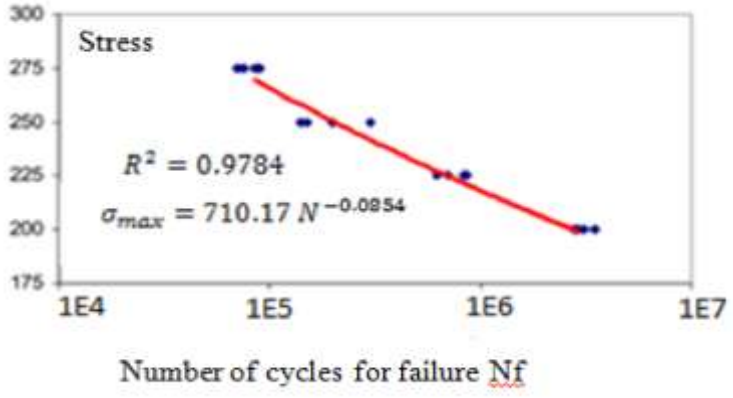

Figure 3: S-N curve for equal biaxial test [10]

E(GPa)	Re(MPa)	Rm(MPa)	HV	K	n
72.5	290	337	11.5	440	0.08

Table 2: Mechanical properties of aluminum (Al-6082-T6)
E : Young Modulu's; Re : Yield stress; Rm: ultimate tensile strength; Ar: Elongation; HV : Hardness Vickers

3.1.2 Numerical results with the simplified approaches
The numerical results are obtained by using the following tools:

- The first simplified approach: CASTEM : A computer code for the analysis of structures by the finite element method. The program is characterized by the exceptional flexibility of the high level macro-language, GIBIANE, so that the user is able to adapt or extend the GIBIANE script to solve any type of finite element problem.
- The second simplified approach: VPS: Virtual Performance Solution is a global solution for Virtual Product Engineering that has its origins in PAM-CRASH, and takes into account multiple domains

Figure 4 shows the analyzed structure with its central thickness variation.

Figure 4: The analyzed structure obtained with VPS software.

The damage initiation and propagation is shown for the two simplified approaches (figures 5). The equivalent stress of Sines is calculated by applying one cycle loading (figure 6).

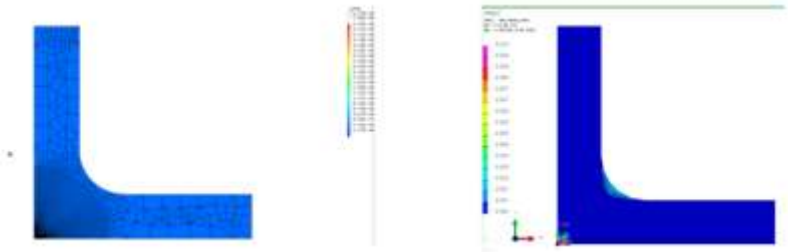

Figure 5.a Step 1: N=2E5 cycles
First simplified approach (Cast3m) 2sd simplified approach (VPS)

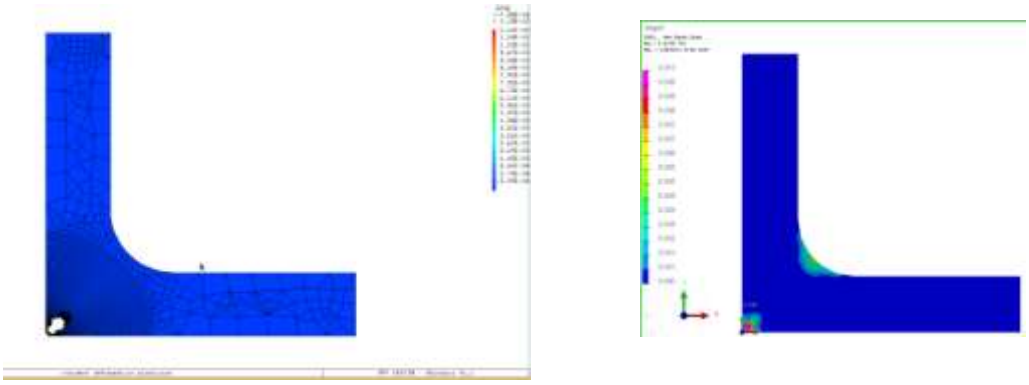

Figure 5.b Step 2: N=3E5 cycles
First simplified approach (Cast3m) 2sd simplified approach (VPS)

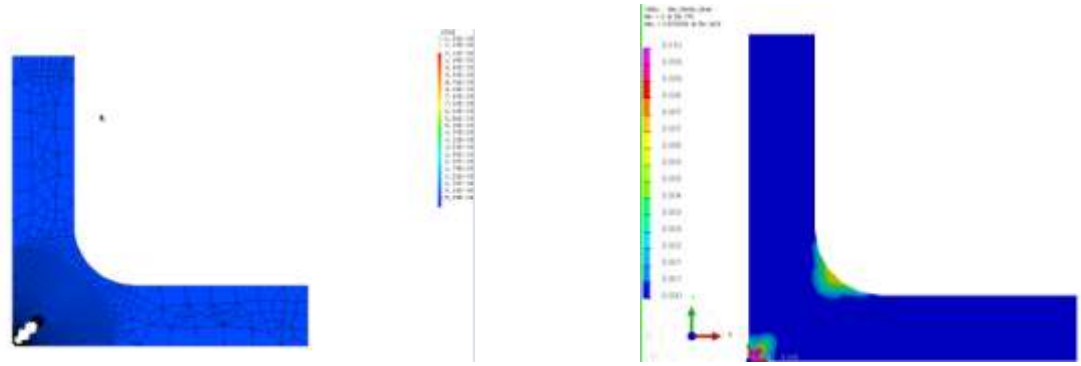

Figure 5.c Step 3: N= 4E5 cycles
First simplified approach (Cast3m) 2sd simplified approach (VPS)

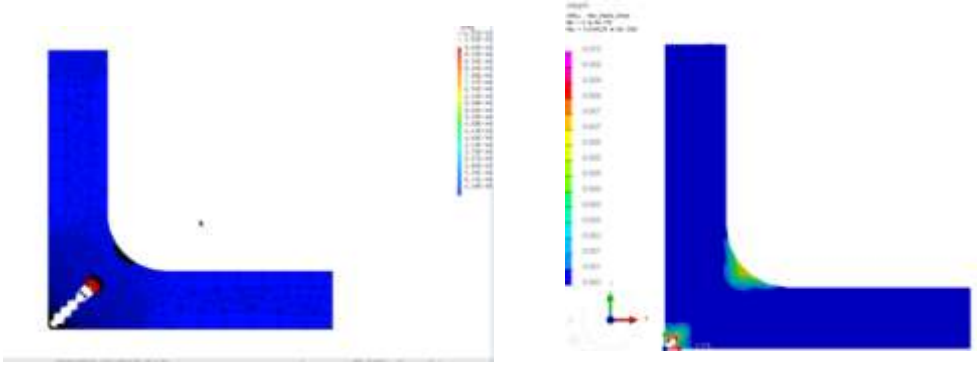

Figure 5.d Step 4: N= 5E5 cycles
First simplified approach (Cast3m) 2sd simplified approach (VPS)

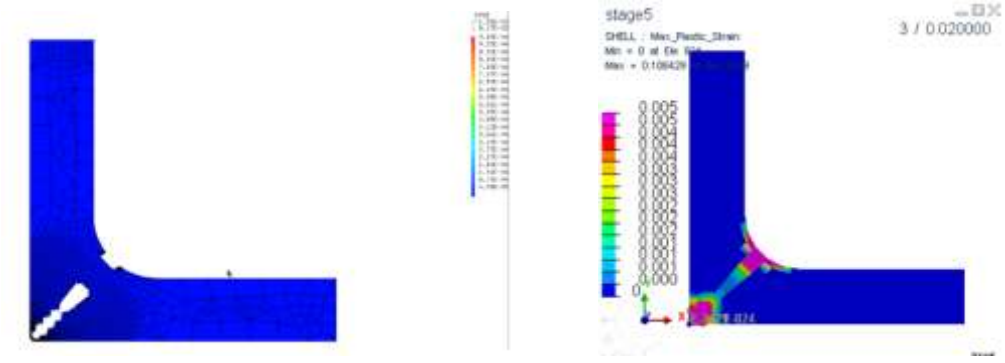

Figure 5.e Step 5: N= 6E5 cycles
First simplified approach (Cast3m) 2sd simplified approach (VPS)

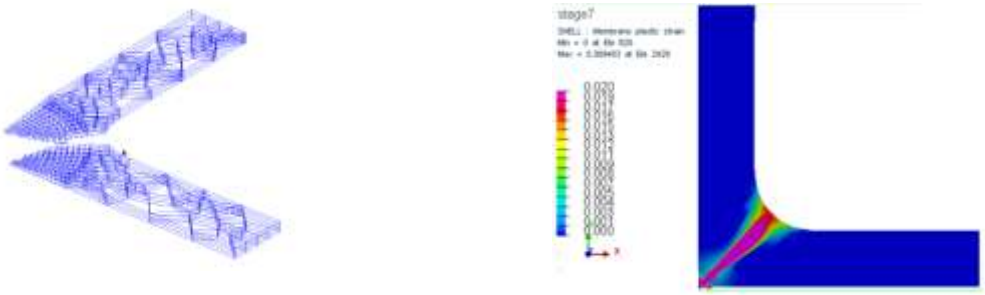

Figure 5.f Step 6: N=7E5 cycles
First simplified approach (Cast3m) 2sd simplified approach (VPS)
Figure 5. Initiation, propagation and structural failure by fatigue

Using the second simplified approach with the jumping model, the results are shown in figure 7 to figure 11.

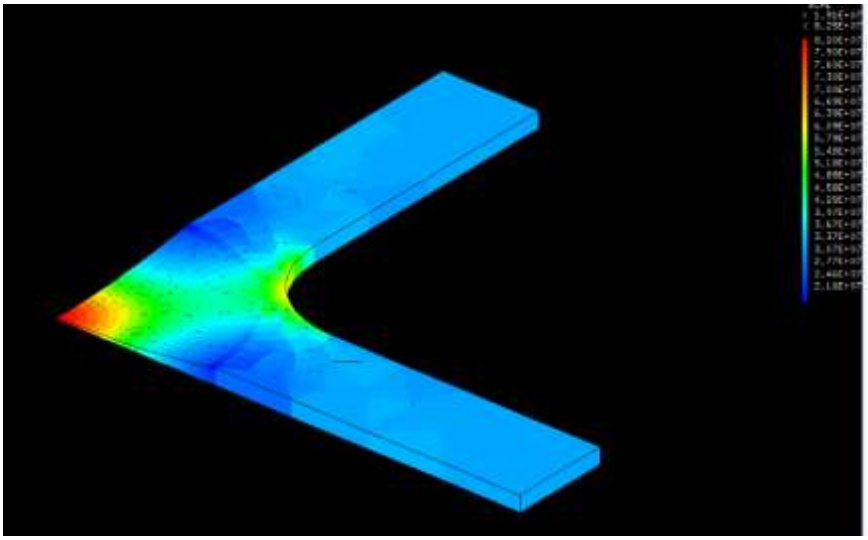

Figure 6: Equivalent Stress of Sines σ_{eqS}

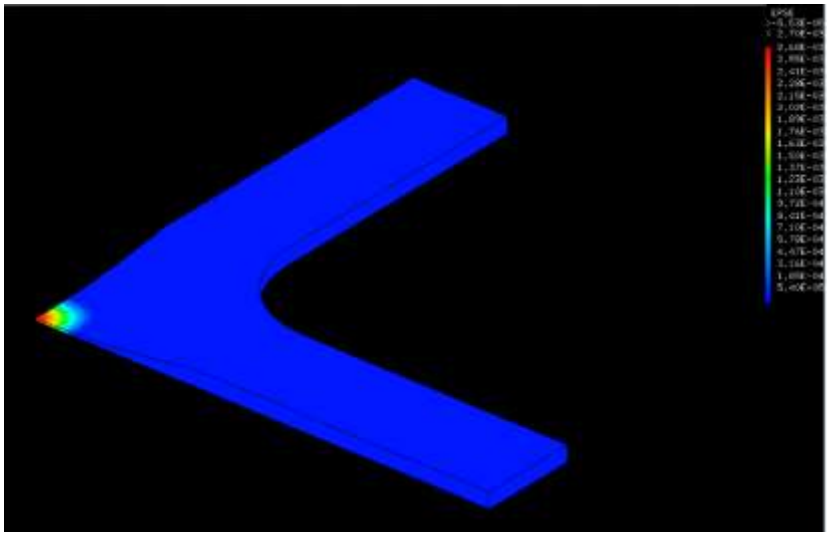

Figure 7: Damaged area at Step 1: N= $3.60357^{E}5$ σ_y =$1.70313^{E}8$ Pa

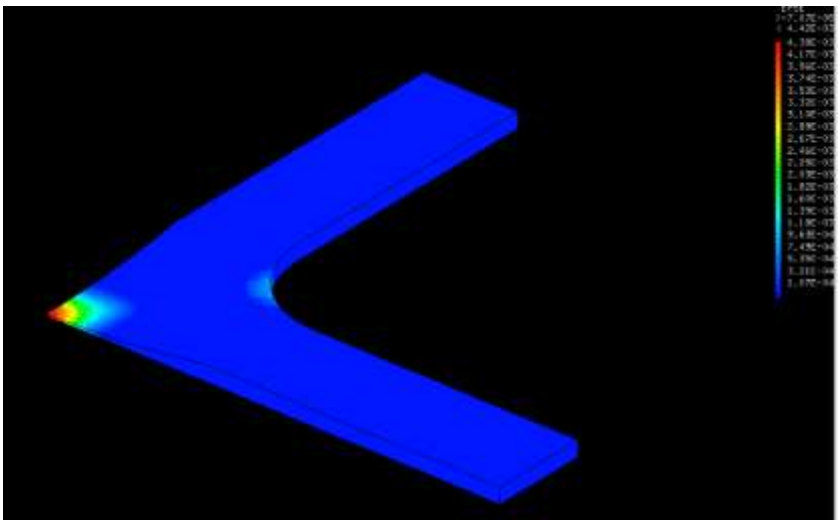

Figure 8: Damaged area at Step 2: N= 5.20288E5 σ_y =1.52952E8 Pa

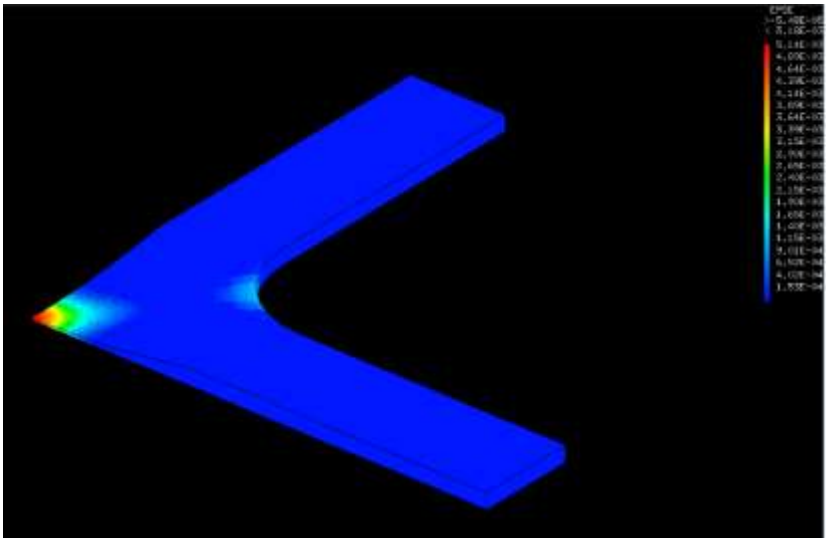

Figure 9: Damaged area at Step 3: N=6.40232E5 σ_y =1.46357E8 Pa

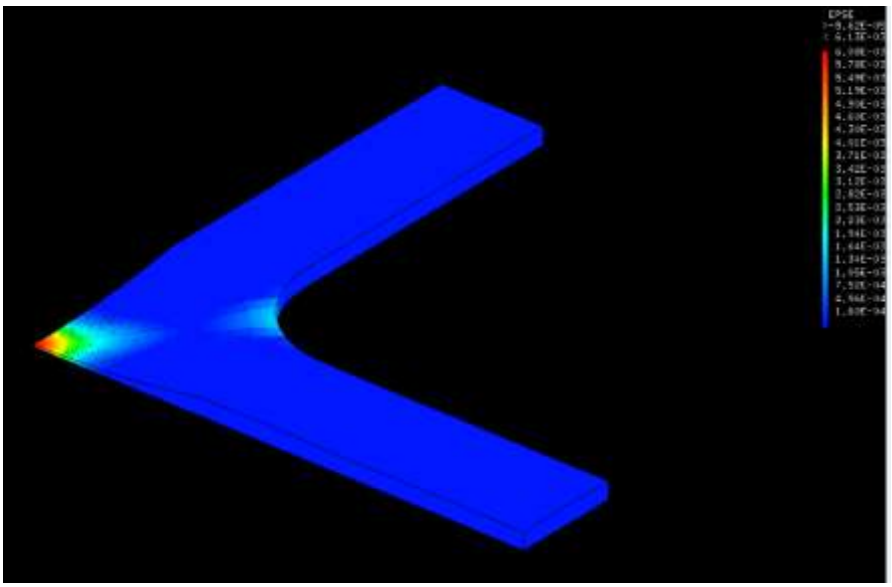

Figure 10: Damaged area at Step4: N=7.30185E5 σ_y =1.42081E8 Pa

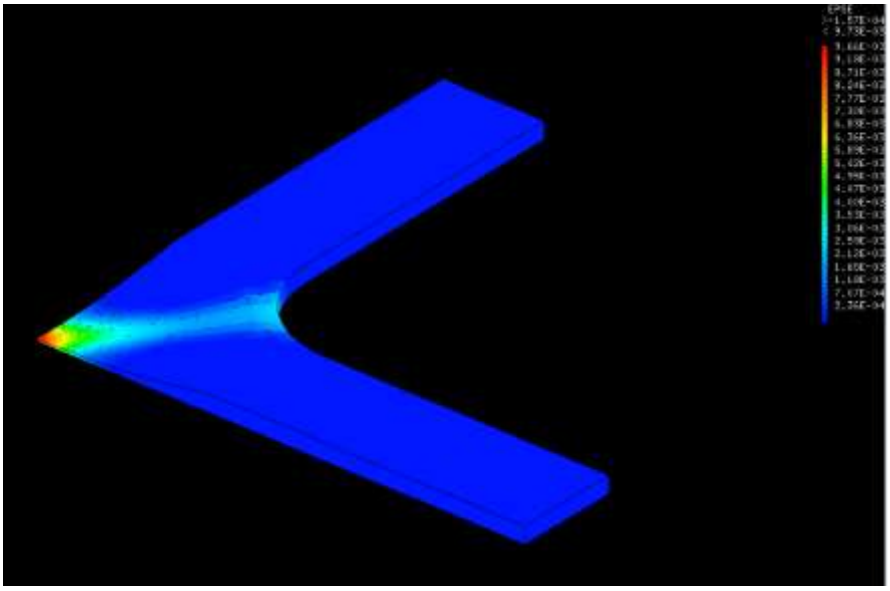

Figure 11: Damaged area at Step 5: N= 7.87647E5 σ_y =1.40524E8 Pa

Using the jumping model, the number of cycles and the associated equivalent stress are illustrated in table 3.

Jumping cycle	2.13252E5	1.59932E5	1.19943E5	89954	57462
N cycles	3.60357E5	5.20288 E5	6.40232E5	7.30185E5	7.87647E5
Equivalent stress(Pa)	1.70313E8	1.52952E8	1.46357E8	1.42081E8	1.40524E8

Table 3: The jumping cycle of the cruciform

The lifetime of this structure is $7.87647 \ \ 10^5$ cycles.
From results, the initiation damaged zone begins in the central area and the damage propagates from the central to the corner areas. Figure 12 shows the experimental initiation –propagation of damage and the structure failure.
When experimental results are compared to numerical ones, we can conclude that :

- The Beginning of the damage fatigue:
- ✓ Experiment result: $N_o = 1.60984 \ \ 10^5$ cycles
- ✓ Present approach: $N_o = 1.47105 \ \ 10^5$ cycles
- The propagation line: from the center to the corner zone; the same experimental and numerical results are observed.
- Final structural failure:
- ✓ Experiment result: $N = 7.49145 \ \ 10^5$ cycles
- ✓ Present approach: $N = 7.87647 \ \ 10^5$ cycles
- Using the Dang Van criterion, the mapping of criterion is represented in figure 13. It follows the same numerical results.

As a conclusion for the simplified approaches: the initiation area and cycle's number of damage, propagation line and the structure's lifetime are well estimated.

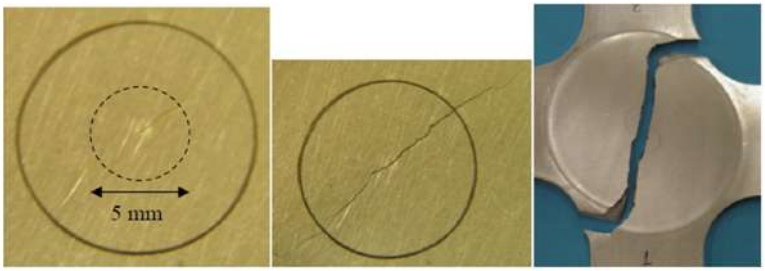

Figure 12: Experimental initiation- propagation and failure of the structure [10].

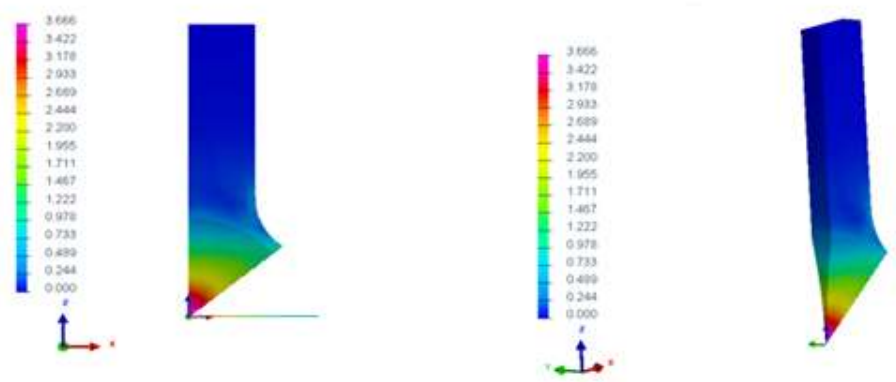

Figure 13: Dang Van mapping

3.4 Industrial example

An industrial example, with a 3D complex geometry subjected to non-symmetric load, is investigated. The considered model deals with the fatigue of the blades of a wind turbine (Electricité De France EDF), proposed by the ESI-Group society (figure 14.a). The material used in this example is 42CrMo4v-steel non corroded. The characteristics of this material are: Rm = 750N/mm²; Surface roughness factor Ks = 0.9; Fatigue limits in reversed bending 398MPa; Fatigue limit in reversed torsion is 260 MPa;

The S-N curve of this material is presented in the figure (figure 14.b). The load applied is multiaxial loading in Y and Z directions. The figure 14.c presents the load in the Y direction. The second simplified approach is used and the different steps of propagation are shown in figure 15 to figure 18. The Dang Van mapping is showed in the figure 19.

The observed lifetime of the structure is $5\ 10^7$ cycles and present approach one is $4.5\ 10^7$ cycles. The initiation and the propagation of the damages obtained with the developed approach are well compared to Dang Van results (Figure 19 can be compared with the figure 17).

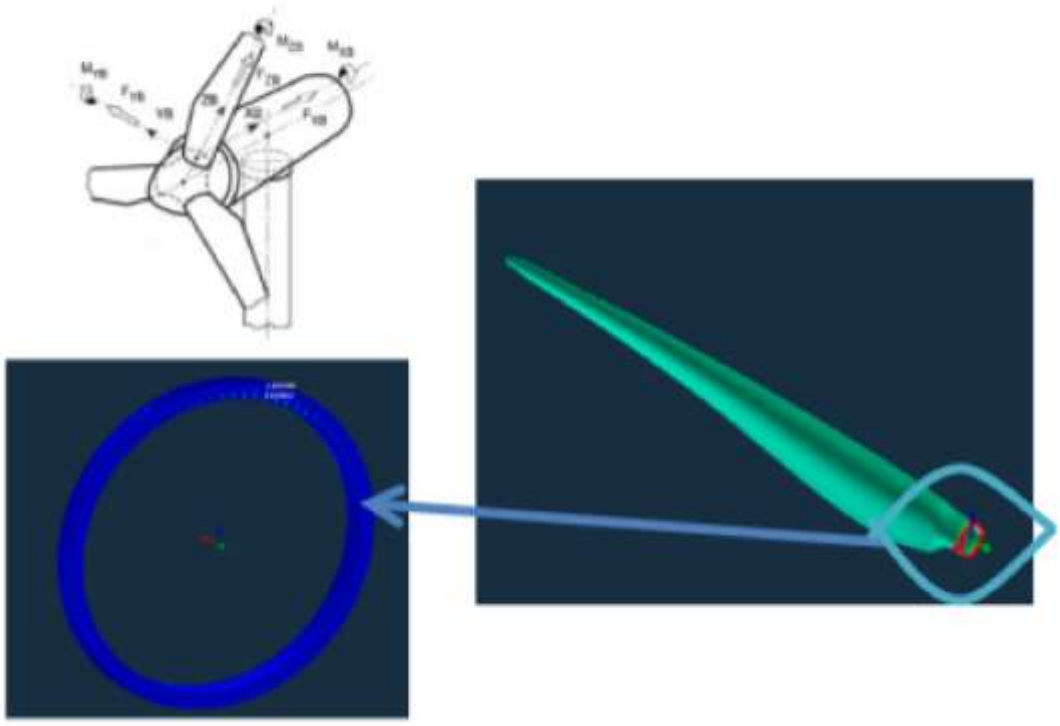

Figure 14.a: The industrial example

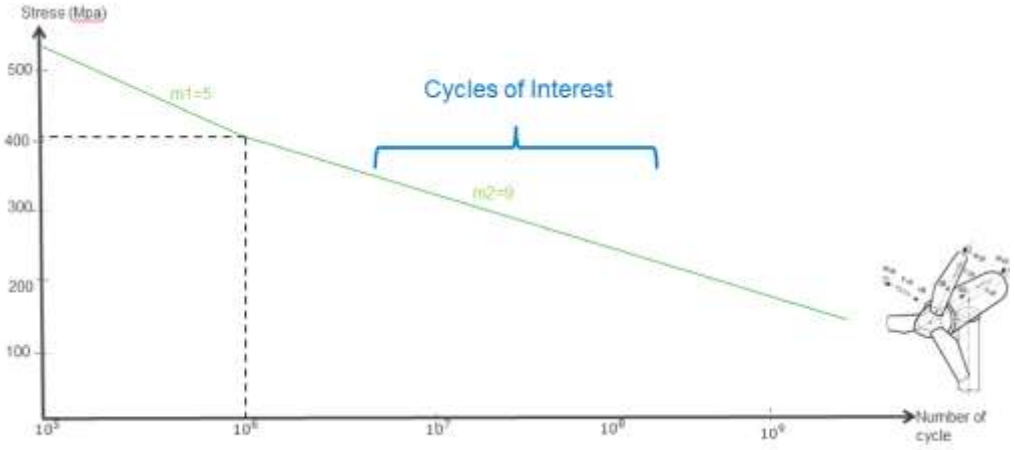

Figure 14.b: S-N curve of steel 42CrMo4v steel

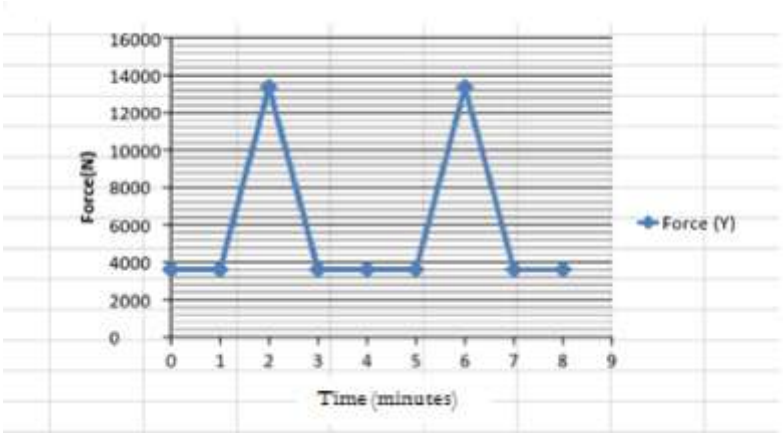

Figure 14.c: cycle loading in Y direction

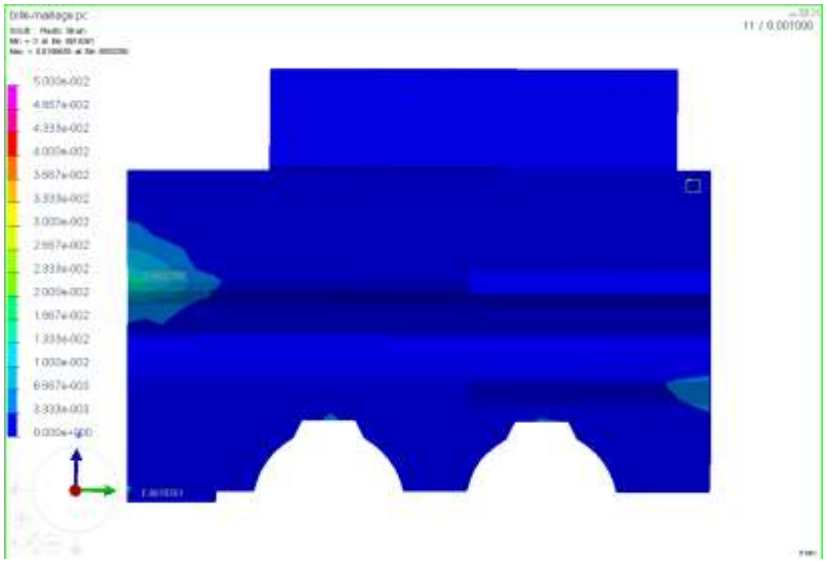

Figure 15: Damaged area at Step 1: σ_y =4E8 Pa; N=1125797=1.13E6 cycles

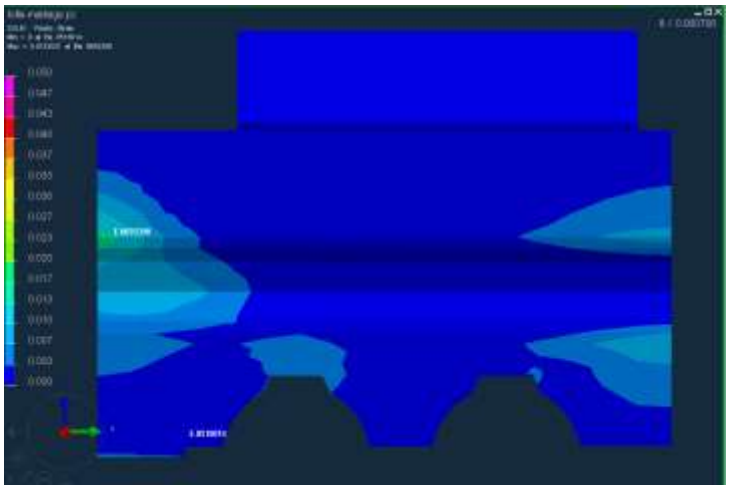

Figure 16 Damaged area at: σ_y =3.6E8 Pa; N= 2.79^{E}7 cycles

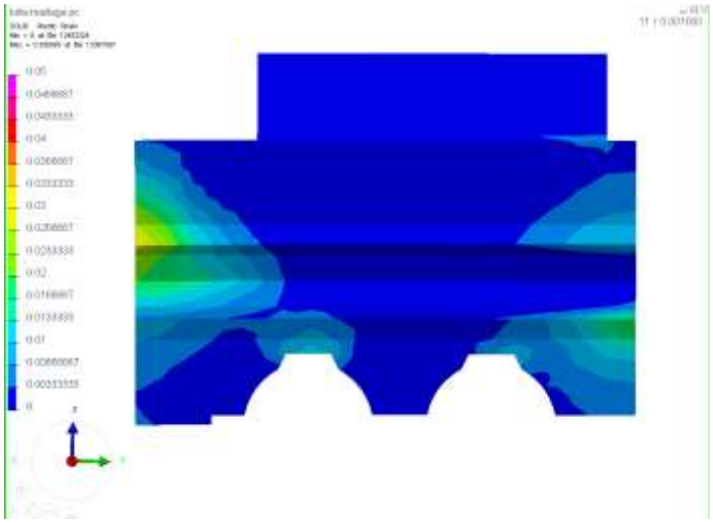

Figure 17: Damaged area at: σ_y =3.2 E 8 Pa ; N=3.87E7 cycles

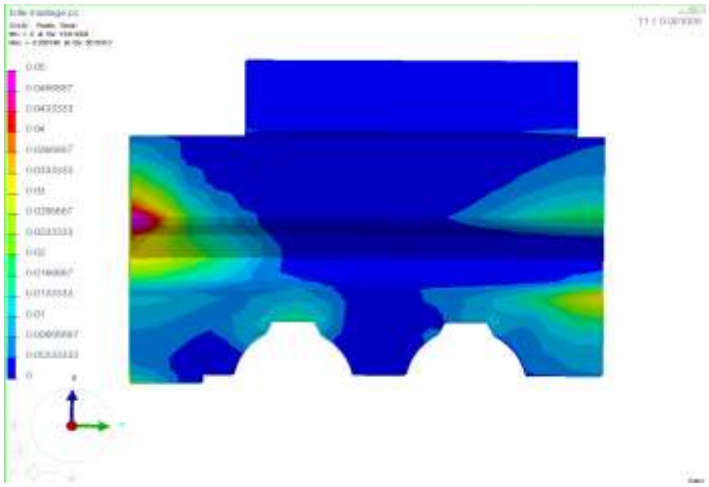

Figure 18: Damaged area at σ_y = 3E8 Pa ; N= 4.579E7 cycles

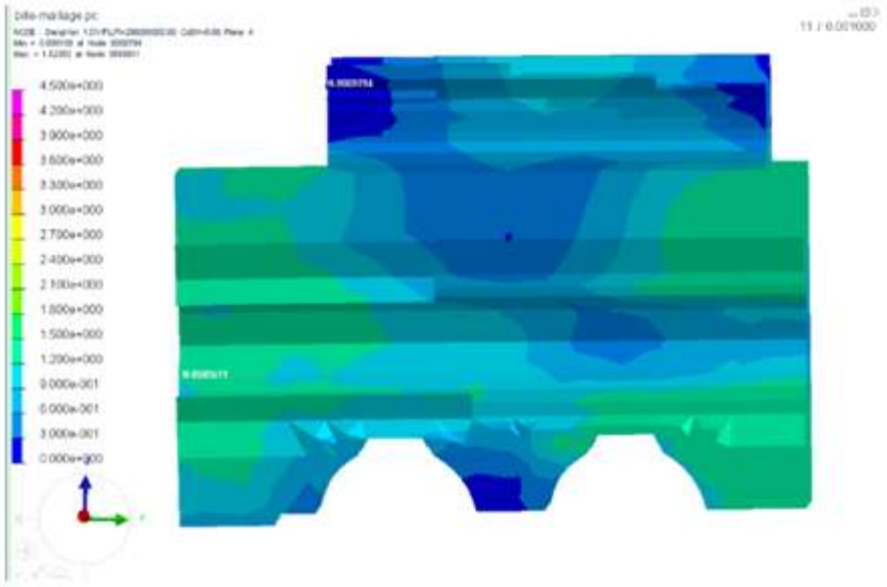

Figure 19: Results obtained with the Dang Van criteria

IV. Conclusion

The proposed approach can be useful in the engineering field to determine the initiation-propagation of the damage and the failure of a structure with a low computational cost.

The approach is based on anisotropic stiffness degradation and a non-homogenous material properties evolution and distribution. This evolution depends on a criterion and its gradient. Each material point stress state is associated to a point of S-N Wöhler curve.

A global two simplified approaches, describing the initiation-propagation damage and the structural failure by fatigue, are presented and used. Two numerical applications are presented to illustrate the simplified approaches: an academic cruciform specimen and an industrial case: blades of a wind turbine of "Electricité De France, EDF". Results show a good agreement of the initiation and the propagation of the fatigue damage with experimental data. The structural failure is well estimated. Results are also compared to the Dang Van mapping. The good agreement of the simplified approaches is encouraging to develop a numerical tool for the general approach.

Appendix: Parameters related to fatigue

A.1. Fatigue Failure Parameters

Since fatigue is a material failure under cyclic loading, special parameters are required for the description of the process. Consider a time dependent, cyclic stress applied to a component, with σ_{max} and σ_{min} being the maximum and minimum levels, respectively. Meaningful parameters are:

- the stress amplitude: $\sigma_a = \frac{\Delta\sigma}{2} = \frac{\sigma_{max} - \sigma_{min}}{2}$ (A.1)
- the mean stress: $\sigma_m = \frac{\sigma_{max} + \sigma_{min}}{2}$ (A.2)
- and the stress ratio: $R = \frac{\sigma_{min}}{\sigma_{max}}$ (A.3

A.2. The S − N Plot

The resistance to fatigue failure, measured by the number of load cycles to failure, is directly related to the stress level. Plots of the stress level (S) versus the number of cycles to failure N_f (in a logarithmic scale) quantitatively describe the relationship and are called S − N curves. Fatigue failure occurs in the most material of sufficiently large values of N regardless of the value of S. Same materials, particularly ferrous alloys, exhibit a threshold stress level (the so called endurance limit) below which fatigue does not take place. As it could be expected, the mean stress level affects the fatigue strength. If stress cycles involve tension and compression of equal magnitudes $\sigma_m = 0$, the stress amplitude associated with failure after N_f load cycles under such condition is

called σ_0. If the stress cycling involves $\sigma_m > 0$, the stress amplitude associated with failure (at the same value of N_f) is smaller and various empirical relationships have been proposed to quantify this behavior.

A.3. Fatigue Lifetime

Fatigue failure can be regarded as the result of material damage accumulation [1]. A simple model of the damage accumulation process is obtained by assuming that each load cycle produces the same amount of damage to the material. This is called the Palmgren-Miner rule of linear cumulative damage. Using this assumption, fatigue lifetime under variable stress amplitude conditions can be estimated from the measured lives under various distinct but constant stress amplitudes. If n_i is the number of cycles spent at stress amplitude σ_a, and N_i is the fatigue lifetime at that same stress amplitude, and the corresponding lifetime fraction is defined as:

$$f_i = \frac{n_i}{N_i} \tag{A.4}$$

A.4. Fatigue criteria

Since 1935, when Gough [9] suggested ellipse quadrant and ellipse arc equations, a great number of multi-axial fatigue criteria have arisen. At the same time, several propositions for their division were suggested. Fatigue criteria can be divided into three groups:

• Empirical criteria
• Critical plane approach criteria
• Global approach criteria.

Nevertheless, this classification is not precise as some criteria could belong to one category when certain aspects are considered and to another one from the point of view of other aspects. This division makes the analysis of some interesting criteria characteristics easier. For more information about fatigue criteria, the following references can be consulted [2-9].

Acknowledgements

The authors are grateful to ESI Group for their help and support.

References

[1] Morel F., Ranganathan N., Petit J., Bignonnet A. (1997). A mesoscopic approach for fatigue life prediction under multiaxial loading. *Proceedings of the 5th International Conference on Biaxial/Multiaxial Fatigue and Fracture*, Edited by E. Macha, Z. Mróz, Technical University of Opole, Opole, 1, 155-172

[2] Carpinteri A. , Spagnoli A. (2001). Multiaxial high-cycle fatigue criterion for hard metals: *International Journal of Fatigue* 23 pp. 135-145.

[3] McDiarmid D. L. (1994). *Fatigue Fracture Engng. Material and Structure*. 14, No. 4 pp. 429-453; and Fatigue Fracture Engng. Mater. Struct. 17, No. 12 pp. 1475-1484.

[4] Sines G., Ohgi G. (1981). Fatigue criteria under combined stresses or strains. *ASME Journal of Engineering Materials and Technology*, 103, 82-90

[5] Dang Van K., Griveau B., Message O. (1989). On a new multi-axial fatigue limit criterion: theory and application, Biaxial and Multi-axial Fatigue, EGF 3, Edited by M.W. Brown and K.J. Miller, Mechanical Engineering Publications Limited, London, 479-496

[6] Crossland B. (1956) Effect of large hydrostatic pressures on the torsional fatigue strength of an alloy steel. Institution of Mechanical Engineers. *International Conference on Fatigue on Metals, London*, pp. 138-149.

[7] Papadopoulos I.V. (1995). A high cycle fatigue criterion applied in biaxial and triaxial out-of-phase stress conditions. *Fatigue and Fracture of Engineering Materials and Structures*, 18, 1, 79-91

[8] Papadopoulos I.V. (1997). A comparative study of multi-axial high-cycle fatigue criteria for metals. *International Journal of Fatigue*, 3, 219-235

[9] Gough H.J. (1950). engineering steels under combined cyclic and static stresses, Transaction of the ASME, *Journal of Applied Mechanics*, 72, 113-125

[10] Chen, S. (2012). Contribution à l'étude du cumul de dommage en fatigue multiaxiale. LILLE-France, L'université Des Sciences Et Technologies De Lille.

[11] Miner, M. A. (1945). Cumulative damage in fatigue. *Journal of Applied Mechanics*, 67,

[12] A159-A164.

[13] Krajcinovic D. (1985). "continuum Damage. Mechanics revisited: basic concepts and difinitions*", journal of Applied Mechanics*, 52 829-834

[14] Krajcinovic D. (1989) Damage Mechanics, Mech Mater., 8 117-197.

[15] SAANOUNI K. (1978). Damage in metal forming, series editor Pierre DEVALAN

[16] 15.Lemaitre J. , Chaboche J.L. (1978). Aspect phénoménologique de la rupture par endommagement, *J. Mec. Appl* 2 167-189

[17] Murakami S. , Ohno N.(1978). A constitutive equation of creep damage in polycrystalline metals, IUTAM Colloquium Euromech 111, Marienbad.

[18] Murakami S. , Ohno N. (1980). A continuum theory of creep and creep damage, 3rd IUTAM Symp on Creep in Structures, Leicester.

[19] Murakami S. (1982). Notion of continuum damage mechanics and its application to anisotropic creep damage theory, *ASME Pressure Vessel and Piping Int. Conf., Orlando*.

[20] Chaboche J.L. (1979). Le concept de contrainte effective appliqué à l'élasticité et à la viscoplasticité en présence d'un endommagement anisotrope, Coll. Euromech 115, Grenoble, (CNRS, 1982).
[21] Chaboche. J.L. (1984). Anisotropic creep damage in the framework of continuum damage mechanics. Nuclear Engineering and Design 79 309-319 309 North-Holland, Amsterdam.
[22] Mazars J. (1979). Application de la mécanique de l'endommagement au comportement non linéaire et à la rupture du béton de structure. Thèse de doctorat, Université de Paris 6.
[23] CHABOCHE J.L. Continuous damage mechanics - A tool to describe phenomena before crack initiation. Nuclear Engineering Design, Vol. 64, 1981, pp. 233-247.
[24] Krajicinovic D. (1985) Continuous damage mechanics revisited: basic concepts and definitions. *J. Applied Mech*. 52 829-834,
[25] Cordebois J.-P. et Sidoroff J.P. (1982). Endommagement anisotrope en élasticité et plasticité. *J.M.T.A.* - Numéro Spécial, 45-60.
[26] Godard V. (2005). *Modélisation de l'endommagement anisotrope du béton avec prise en compte de l'effet unilatéral: Application à la simulation des enceintes de confinement nucléaires*. Phd Thesis of Pierre and Marie Curie University.
[27] Hansen N.R., Shreyer H.L. (1995). Damage deactivation. ASME *J. Applied Mechanics*. 62, 450-458.
[28] Ekh M., Menzel A., Runesson K.,Steinmann P. (2003). Anisotropic damage with the MCR effect coupled to plasticity. *International Journal Engineering Sciences*, 41, 1535-1551.
[29] Kachanov, L., 1958. On the Time to Fracture under Conditions of Creep. Izv. AN SSSR. Otd. Tekh. Nauk, pp. 26–35.
[30] Rabotnov, Y.N., 1963. Paper 68: On the equation of state of creep. In: Proceedings of the Institution of Mechanical Engineers. Conference Proceedings, vol.
[31] 178. SAGE Publications, pp. 2–117.
[32] Lemaitre, J., Chaboche, J.-L., 1978. Aspect phénoménologique de la rupture par endommagement. J. Mec. Appl. 2.

A. Manai. "A pragmatic anisotropic Damage Fatigue Model Based on a failure criterion and its gradient ." IOSR Journal of Mechanical and Civil Engineering (IOSR-JMCE) , vol. 14, no. 5, 2017, pp. 56–73.